RSC Advances

PAPER

View Article Online
View Journal | View Issue

Cite this: *RSC Adv.*, 2021, **11**, 18231

Sabina chinensis leaf extracted and *in situ* incorporated polycaprolactone/polyvinylpyrrolidone electrospun microfibers for antibacterial application

Yan Ge, [abc] Jiapeng Tang, [de] Azeem Ullah,[c] Sana Ullah,[c] Muhammad Nauman Sarwar[c] and Ick-Soo Kim *[c]

Sabina chinensis is a valuable reforestation conifer and traditional medicinal plant. In order to retain the physiological and pharmacological activities of the plant and obtain a fibrous material with better antibacterial properties, a mixed solvent of dichloromethane and *N*,*N*′-dimethylformamide was used to obtain the leaf extracts, and *Sabina chinensis* leaf extract (ScLE)-loaded PCL/PVP microfibers were successfully fabricated by electrospinning. The whole preparation process was carried out at room temperature to avoid deterioration of active ingredients. From the antibacterial activity test, it was observed that ScLE-loaded polycaprolactone/polyvinylpyrrolidone (PCL/PVP) microfibers had potential antibacterial activity against both Gram-positive and Gram-negative bacteria stains. The morphological properties of the prepared microfibers were observed by SEM. As the proportion of ScLE increased, the fiber diameter gradually increased and the surface was smooth. The excess ScLE addition caused the formation of beads during electrospinning. Considering different characterization results, 33% (v/v) addition of ScLE to the spinning solution was the optimum ratio. The winding structure obtained by the interaction of components in ScLE with PCL and PVP was confirmed by FTIR, XRD and WCA tests, which indicated that ScLE-loaded microfibers possessed excellent thermal stability, tear resistance and degradation resistance. It is expected that the prepared composite microfibers have potential applications as robust antibacterial meshes and films in the fields of biomedicine and air purification.

Received 8th February 2021
Accepted 28th April 2021

DOI: 10.1039/d1ra01061a

rsc.li/rsc-advances

1. Introduction

Sabina chinensis (L.) Ant, an evergreen tree of the family Cupressaceae, which is mostly distributed in East Asia, is a valuable reforestation conifer and traditional medicinal plant.[1] It has two forms of leaves, namely scaly leaves and spiny leaves. The two types of leaves of *Sabina chinensis* are rich in terpenoids, including sabinene, limonene, β-pinene, bornyl acetate, phellandrene, *p*-menth-1-en-4-ol and cedrol, and flavonoids, including amentoflavone, hinokiflavone and apigenin.[2–4] The Compendium of Materia Medica recorded that *Sabina chinensis* can be used as a diuretic to fight inflammation and relieve congestion and can contribute to regulation of blood sugar levels. It is very helpful to treat asthma, bladder infection, fluid retention, gout, obesity and prostate disease.[5,6] The leaf extract of *Sabina chinensis* also exhibits mosquito repellent and antitumor effects.[7,8] In addition to afforestation and medicinal purposes, the cedarwood oil and cedrol extracted from *Sabina chinensis* are the main bioactive components of this plant, and they are widely used in woody, spicy and oriental flavors for disinfectants and sanitary products. Previous experiments have confirmed that volatile oil from *Sabina chinensis* (L.) Ant leaves has great bacteriostatic and bactericidal effects on *Staphylococcus aureus*, *Staphylococcus epidermidis* and *Escherichia coli*.[9] Experimental data have demonstrated that limonene and β-pinene in the volatile oil can significantly inhibit airborne bacterial growth and they may be the main active ingredients for bacteriostasis and sterilization.[2]

The discovery journey of artemisinin shows that some natural products lose their physiological activity after heat treatment.[10] Many volatile terpenoids with C=C bonds and phenolic hydroxyl groups in their skeletons are unstable and susceptible to deterioration in the presence of oxygen, light and

[a]*School of Textile and Clothing, Nantong University, Nantong 226019, PR China*
[b]*National & Local Joint Engineering Research Center of Technical Fiber Composites for Safety and Protection, Nantong University, Nantong 226019, PR China*
[c]*Nano Fusion Technology Research Group, Division of Frontier Fibers, Institute for Fiber Engineering IFES-Interdisciplinary Cluster for Cutting Edge Research ICCER, Shinshu University, Tokida 3-15-1, Ueda, Nagano 386-8567, Japan. E-mail: kim@shinshu-u.ac.jp*
[d]*Department of Physiology and Hypoxic Biomedicine, Institute of Special Environmental Medicine, Nantong University, Nantong 226019, PR China*
[e]*Co-innovation Center of Neuroregeneration, Nantong University, Nantong 226001, PR China*

temperature.[11] To maximize the utility of natural extracts and prevent their deterioration, they should be preserved by blending them with other delivery chemicals without heating.

As a simple and the oldest technology, electrospinning can produce micro- and nanofibers with smooth and homogenous morphology. The electrospun fibers can be applied in biomedicine, pharmacy, food, water treatment, air purification, energy electronics and information engineering.[12–21] The electrospun fibers can be fabricated using natural polymer or synthetic polymer as the main substrate materials and the appropriate solvents based on these different fields. The preparation process shows a greater deal of autonomy and plasticity. In particular, a non-heating process can be realized during the electrospinning process, which is beneficial to protect natural products and maintain their physiological activity.

Polycaprolactone (PCL) is a biopolymer that is easily soluble in many polar organic solvents. Due to its good film-forming ability, biocompatibility and non-toxicity, PCL is widely used as a medical biodegradable material and drug delivery system.[22,23] PCL materials have certain rigidity and strength and good compatibility with other polymers; they can also be used as modifiers to improve some properties of other polymers.[24,25] In addition, PCL shows good flexibility, and its products possess great characteristics of shape memory.[26,27] The high hydrophobicity and low biodegradation rate of PCL limit its application in the biomedical field.[28,29] As a synthetic water-soluble polymer, polyvinylpyrrolidone (PVP) has excellent colloidal protection, film-forming, adhesion, hygroscopicity, solubilization and coagulation properties.[30] PVP can be dissolved in both water and most organic solvents, and it displays low toxicity, good biocompatibility and appropriate viscoelastic properties, which are also rare in biopolymers.[30,31] The hydrophilicity and biodegradability of electrospun PCL micro- and nanofibers are improved by incorporating PVP into PCL organic solution.[28,29,32–37]

In this study, the solution extracted from fresh leaves of *Sabina chinensis* by organic solvent at room temperature was directly used as the spinning solvent. PCL and PVP were directly added to the spinning solvent to prepare the spinning solution. *Sabina chinensis* leaf extract (ScLE)-loaded PCL/PVP microfibers were fabricated by electrospinning. The surface morphology, mechanical performance, thermal properties, degradability and antibacterial activity of the microfibers were characterized to assess the potential of ScLE in combination with PCL/PVP microfibers, which will provide a robust and compatible solution for the efficient utilization of natural extracts.

2. Materials and methods

2.1. Materials

PCL (average M_n = 80 000) and PVP (average M_w = 1 300 000) were purchased from Sigma-Aldrich Co., Ltd. Dichloromethane (DCM) and *N*,*N*-dimethylformamide (DMF) were purchased from Wako Chemicals Co., Ltd. All the reagents were used as received without further purification. The fresh leaves of *Sabina chinensis* were obtained from the Faculty of Textile Science and Technology in Shinshu University, Tokida, Ueda, Nagano, Japan.

2.2. Preparation of ScLE

500 g fresh leaves of *Sabina chinensis* cut into 0.5–1 cm segments were divided into 5 pieces. The leaf fragments were impregnated into 200 ml of a reagent mixture of DCM and DMF (4 : 1 v/v) and then stirred in a sealed container at room temperature for 24 h in turns. The mixture was filtered with crude filter paper followed by ADVANTEC No. 5C paper to obtain the clarified filtrate as ScLE for electrospinning.

2.3. Preparation of ScLE-loaded PCL/PVP microfibers

The ScLE was mixed with the mixture reagents of DCM and DMF (4 : 1 v/v) in volume ratios of 25 : 75, 33 : 67, 50 : 50 and 100 : 0 to prepare a series of mixed solvents containing different concentrations of ScLE. Then, PCL and PVP were dissolved in the mixed solvents to obtain PCL/PVP mixture solutions (PCL, 10% w/v and PVP, 3.2% w/v). The resultant solution was electrospun at a voltage of 12 kV, a distance of 15 cm between the tip and drum collector and a flow rate of 1.2 ml h^{-1}. The rotating speed of the drum collector was 30 rpm. Finally, the prepared ScLE-loaded PCL/PVP microfibers were dried in air for 24 h and placed in sealing bags for subsequent characterization and evaluation. The PCL/PVP microfibers were labeled as ScLE-1, ScLE-2, ScLE-3, and ScLE-4 according to the concentration of leaf extract. PCL/PVP microfibers without added leaf extract were used as a control.

2.4. Characterizations

The surface morphologies of the microfiber samples were observed using scanning electron microscopy (SEM), JSM-6010LA, JEOL Ltd, Japan. Before the SEM observations, the samples were coated with platinum (Pt).

The chemical structures of the microfiber samples were assayed on a Fourier transform infrared (FTIR) spectrometer (JASCO FTIR-6600, Japan). All spectra were collected in transmission mode in the wavelength range of 4000–400 cm^{-1} wavenumbers in a dry atmosphere at room temperature to observe the possibility of any chemical interaction between PCL/PVP and ScLE.

X-ray diffraction (XRD) was used to analyze the crystallization characteristics of the PCL/PVP microfibers and ScLE-loaded PCL/PVP microfibers using nickel-filtered Cu-Kα radiation-assisted XRD diffractometry (Rotaflex RT300 mA, Rigaku Co., Osaka, Japan). The scanning speed was maintained at 5° min^{-1} and the 2θ range was located from 5° to 80°.

The thermal behavior of the electrospun fibers with and without ScLE was examined by a thermal analyzer (Thermo-plus TG 8120, Rigaku Corporation, Osaka, Japan). The samples were heated under normal atmosphere from 30 °C to 600 °C with a heating rate of 10 °C min^{-1}.

The mechanical properties (*i.e.* tensile stress, tensile strain, and Young's modulus) of the microfiber samples were evaluated using a Universal Testing Machine (UTM), Tesilon RTC 250A; A&D Company Ltd., Japan. Five specimens for each sample were

prepared following the ISO 13634 testing standard, and the thickness of the specimens was tested primordially using a manual micrometer with a resolution of 0.01 mm. The test was performed at a crosshead speed of 20 mm min^{-1} in ambient temperature at 24 °C and 65% humidity.

The hydrophilicity of the microfiber samples was analyzed by water contact angle using an automatic contact angle meter (CA-VP, Kyowa Interface Science Co., Ltd., Japan). The water contact angles of the PCL/PVP and ScLE-loaded PCL/PVP microfibers were measured at room temperature using the sessile drop method. Five readings were measured for each sample, and the means were calculated.

2.5. *In vitro* degradation

The resistance of the PCL/PVP microfiber samples to degradation was determined by incubating the specimens with pH 7.4 0.01 M phosphate buffered saline (PBS, Sigma, USA) solution according to our previous report.[38] Briefly, the specimens were immersed in 50 ml sterile PBS solution and incubated at 37 °C for 7 days. The samples were removed from the buffer on day 3 and day 7 and were washed three times with distilled water. After that, the specimens were placed in a vacuum drying oven at room temperature for 24 h. The morphologies and structures of the microfibers were examined by SEM to observe the morphological changes after degradation. The results were analyzed with unpaired *T* tests using GraphPad Prism 8.3.0.

2.6. Antibacterial test

The antibacterial activity of the PCL/PVP microfibers was tested by the disk diffusion method.[39] 10^7 cells per milliliter bacterial suspensions of *S. aureus* ATCC 6538 (Gram-positive) and *E. coli* ATCC 8739 (Gram-negative) were prepared. A 100 μl aliquot of the resultant bacterial suspension was spread onto a nutrient agar plate. All the PCL/PVP microfiber samples were cut into circular discs (10 mm in diameter) and placed on the top of the agar plate, which was then incubated at 37 °C for 24 h. The diameters of the inhibition zones around the specimens were recorded to assess their antibacterial activity.

3. Results and discussion

3.1. Morphology of the PCL/PVP microfibers

Fig. 1 shows the morphologies of the electrospun microfibers of PCL/PVP and PCL/PVP mixed with different proportions of ScLE. The color of the spinning solutions and microfiber films changed from light to dark with increasing proportion of ScLE in the spinning solution. The diameter of the PCL/PVP microfibers without adding ScLE was 2186 ± 472 nm, and their surface was smooth. The diameter of the microfibers with a low ScLE concentration decreased to 1447 ± 498 nm and the observed microfiber surface became rough, which was accordant with the decrease in diameter of chitosan nanofibers by the incorporation of tea tree oil liposomes.[40] This probably occurred because the diameter of the microfibers became small and the concave–convex surface similar to the surface of the PCL/PVP fibers was highlighted. As the ScLE proportion continued to increase, the diameter of the fibers increased to 2621 ± 776 nm and the fiber surface became smooth, which manifested that the ScLE ingredients could be well blended with PCL and PVP. This was consistent with the finding that the fiber diameter increased with the increase of concentration of tea tree oil liposomes incorporated in chitosan nanofibers in another report.[41] Obviously, the influence of ScLE doping on microfiber diameter was nonlinear. The continued increase in ScLE proportion gradually destroyed the blend system, resulting in fiber bifurcation and a rough fiber surface. When 100% (v/v) ScLE was used as a solvent to prepare PCL/PVP microfibers, the

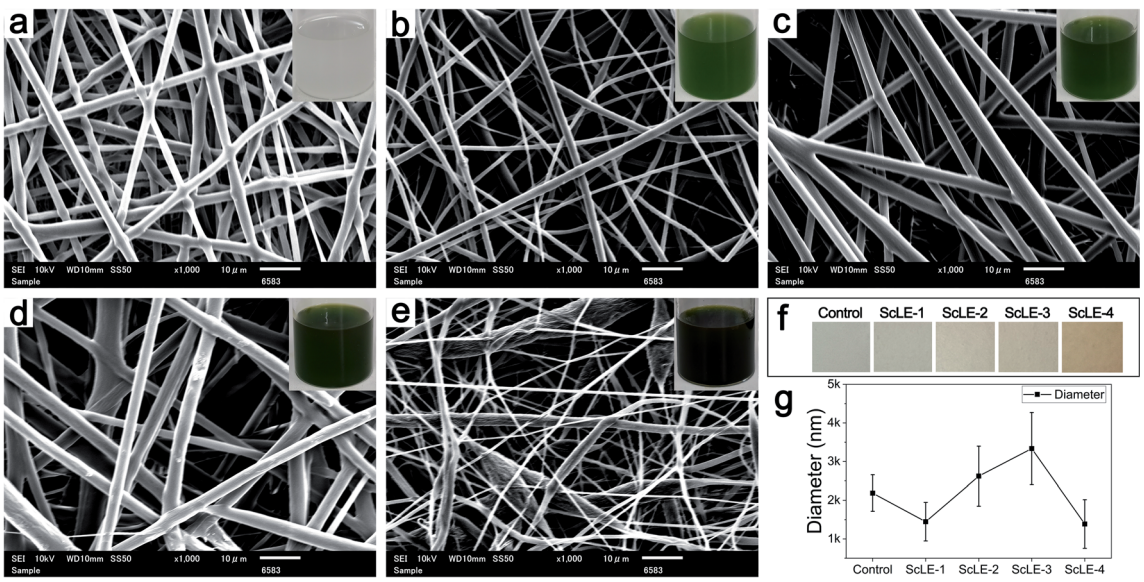

Fig. 1 SEM images of (a) neat PCL/PVP, (b) ScLE-1, (c) ScLE-2, (d) ScLE-3 and (e) ScLE-4 microfibers. (f) The color and texture of the prepared microfiber films. (g) The average diameters of the microfibers.

fibers became very thin and were only 1387 ± 630 nm in diameter, accompanied by numerous beads. These beads were induced by the fact that the electrostatic field could not effectively stretch the spinning solution.[42] Meanwhile, the high electrostatic field force caused enhancement of the electrostatic repulsive force on the liquid jet, which then increased the bead formation on the fibers.[43] The hydrophilic components in *Sabina chinensis* leaves were inevitably incorporated into the spinning solvent during the extraction, which may have affected the stability of the organic solvent system. Moreover, the hydrophilic components in the spinning solution would also hinder the volatilization of the solvent in the electrospinning process, which should be an important reason for the formation of beads.[44,45]

3.2. XRD analysis

XRD studies were performed to confirm the crystalline structures of the neat PCL/PVP and ScLE-loaded microfibers (Fig. 2). It could be observed that the PCL/PVP microfibers presented two characteristic peaks at angles (2θ) of 21.8° and 23.9°, which correspond to the characteristic peaks of PCL.[37] These two peaks slightly shifted towards high angles as ScLE was loaded on the PCL/PVP microfibers. The shifting was consistent with PVA nanofibers containing *Juniperus chinensis* extracts.[46] In addition, the ScLE-1 microfibers with a low added proportion of ScLE exhibited lower intensity compared with the neat PCL/PVP microfibers, which is coincident with the decrease of fiber diameter shown in Fig. 1b. This result indicated that the addition of ScLE destroyed the crystallinity of the PCL/PVP microfibers. With the increase of the ScLE proportion, the intensity of the characteristic peaks continuously increased; however, the full width at half maximum of the angle continued to decrease. The results showed that some components of ScLE formed small grains after solvent volatilization, whose orientation in the fibers was enhanced, and the small grains merged into large grains, causing higher crystallinity.[47] The effect of ScLE addition on the crystal structure of PCL/PVP microfibers displayed that the hydrogen bonds among the macromolecules were broken and then ScLE component crystals were constructed, which is attributed to the new interactions between ScLE and the original macromolecules, PCL and PVP.

3.3. FTIR analysis

FTIR spectra can be used to analyze the specific interactions among molecules in microfibers. Fig. 3 shows the FTIR spectroscopy graphs of the PCL/PVP microfibers, ScLE-loaded PCL/PVP microfibers and ScLE solution. It has been reported repeatedly in the literature that the absorption peaks of PCL/PVP microfibers were located at 2947 cm^{-1}, 2866 cm^{-1} and 1723 cm^{-1}, which were assigned to the stretching vibration of $-CH_2-$ and vibration of –C=O bonds to PCL macromolecules, and at 1667 cm^{-1}, 1420 cm^{-1} and 1291 cm^{-1}, which were assigned to the stretching vibration of C=O, C–C and C–N bonds in the PVP macromolecules.[37,38] The C=O absorption peak of the ScLE solution located at 1667 cm^{-1} may be caused by DMF, and the broad peak at 3500 cm^{-1} indicated that ScLE contained abundant alcohol ingredients, which provided the possibility for the formation of hydrogen bonds between ScLE and PVP molecules. As mentioned in the previous literature, the interactions between PCL and PVP molecules are weak.[37] This may be related to their molecular characteristics. PCL is a hydrophobic macromolecule that is soluble in many polar organic solvents but insoluble in aqueous solution. PVP is a typical hydrophilic macromolecule which has greater solubility in water and most organic solvents. Due to the presence of the lactam group, the molecular structure of PVP approximates to the simple protein model, and it has capability to interact with a wide range of hydrophilic and hydrophilic materials.[48] Therefore, incorporation of the appropriate amount of ScLE did not significantly change the interaction between PCL and PVP molecules, and their infrared absorption peaks were parallel to

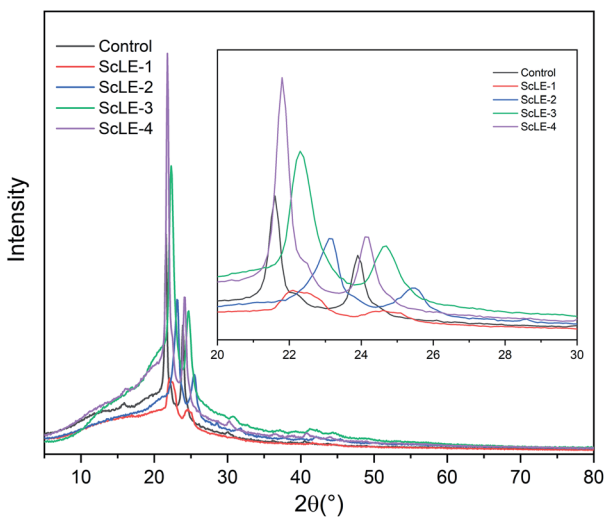

Fig. 2 X-ray diffraction patterns of the neat PCL/PVP, ScLE-1, ScLE-2, ScLE-3 and ScLE-4 microfibers.

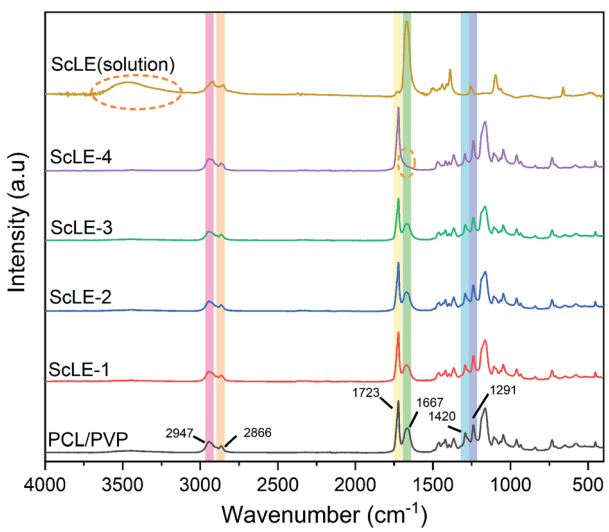

Fig. 3 Comparison of the FTIR spectra of ScLE (solution) and the neat PCL/PVP, ScLE-1, ScLE-2, ScLE-3 and ScLE-4 microfibers.

those of the PCL/PVP microfibers. Notably, the C=O stretching vibration peak at 1667 cm^{-1} in sample ScLE-4 disappeared. This implied that some hydrophilic components in the ScLE formed intermolecular hydrogen bonds with the carbonyl oxygen of PVP. The formation of hydrogen bonds may indicate that the stability of the system in which the solvent volatilized in the spinning solution and the polymer stretched to form fibers was destroyed during the electrospinning process, which coincided with the appearance of considerable beads shown in Fig. 1e. The formation of hydrogen bonds was also related to the increase of grain size in ScLE-4, indicating that the beads were formed by the aggregation of small grains, which was identical to the increase in the diffraction peaks corresponding to the increase of ScLE proportion in Fig. 2.

3.4. The thermal stability of the PCL/PVP microfibers

Thermogravimetric analysis (TGA) is used to investigate the behavior of PCL/PVP microfibers at high temperature. Fig. 4a shows the mass loss of the PCL/PVP microfibers with ScLE during the heating process. At the initial stage of heating (30–100 °C), the mass of PCL/PVP microfibers containing ScLE did not decrease significantly, testifying that the ScLE components were firmly combined with PCL/PVP microfibers. This may be due to the consistency of plant extracts and spinning solvents, which was different from the other fibers prepared by adding plant extracts. Those fibers possessed moisture and highly volatile components; therefore, their TGA plot demonstrated almost the same trend.[39,49] It could be observed that the ScLE-1, ScLE-2, ScLE-3 and PCL/PVP microfibers were thermally stable up to 280 °C and exhibited consistent degradation until 400 °C, where they reached the combustion stage. As shown in Fig. 4b, the maximum rate of oxidative degradation for all samples occurred at 400 °C. The onset temperature for ScLE-4 microfibers occurred at a lower temperature (180 °C) because the amount of ScLE exceeded the encapsulation capacity of PCL/PVP. The ScLE was dissociated and evaporated firstly from the microfibers at temperatures above 180 °C. At the same time, the excess ScLE may have destroyed the intermolecular interaction of the PCL/PVP microfibers, and the rate of mass loss was faster than that of the other microfibers. Therefore, the low thermal stability of the ScLE-4 microfibers can be associated with their loose structure. However, ScLE-1, ScLE-2, ScLE-3 and ScLE-4 all had sufficient thermal stability for antibacterial applications.

3.5. Mechanical properties of the PCL/PVP microfibers

For the aims of biomedicine and air purification, antibacterial fibers should possess adequate mechanical properties, such as strength, toughness, softness and elasticity. Human tissues and organs demonstrate a diversity of mechanical properties. They are mainly divided into soft tissue and hard tissue. Soft tissue includes spinal cord, skin, muscle, brain, serpentine, nanowire on elastomer, metal mesh, endocranium and pericardium, whose Young's moduli range from 1 kPa to 100 MPa.[50] Moreover, antibacterial fiber meshes formed by microfibers are used as filters and barriers for air purification. They also need to possess high mechanical strength under the condition of continuous airflow.[51] Fig. 5 shows the tensile curves and properties of the PCL/PVP microfiber meshes. The Young's modulus of the neat PCL/PVP microfibers was 2.55 ± 0.06 MPa, and the Young's modulus of the PCL/PVP microfibers increased gradually after adding ScLE. The maximum Young's modulus of ScLE-2 was obtained at 4.17 ± 0.14 MPa. This indicated that a small amount of ScLE component crystals could form a benign crystal structure with the PCL/PVP and PVP macromolecules entangled on the ScLE component crystals, which was helpful to improve the rigidity of the fiber. As the ScLE proportion continued to increase, the Young's modulus of the PCL/PVP microfibers gradually decreased. The Young's modulus of ScLE-4 was only 0.27 ± 0.07 MPa when the spinning solvent was completely replaced by ScLE. These results showed that the excess ScLE component crystals combined with PCL/PVP to destroy the original hydrogen bonds among the PCL molecules, resulting in a decrease of the fiber strength. ScLE-2 excelled in terms of ultimate tensile strength among the samples, up to 4.97 MPa.

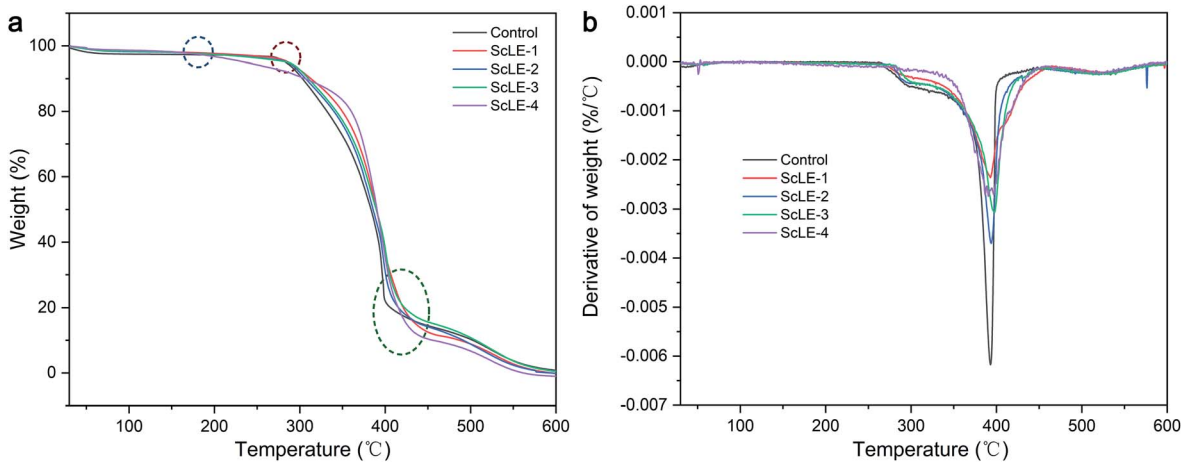

Fig. 4 (a) Thermogravimetric curves and (b) derivative thermogravimetric curves of the neat PCL/PVP, ScLE-1, ScLE-2, ScLE-3 and ScLE-4 microfibers.

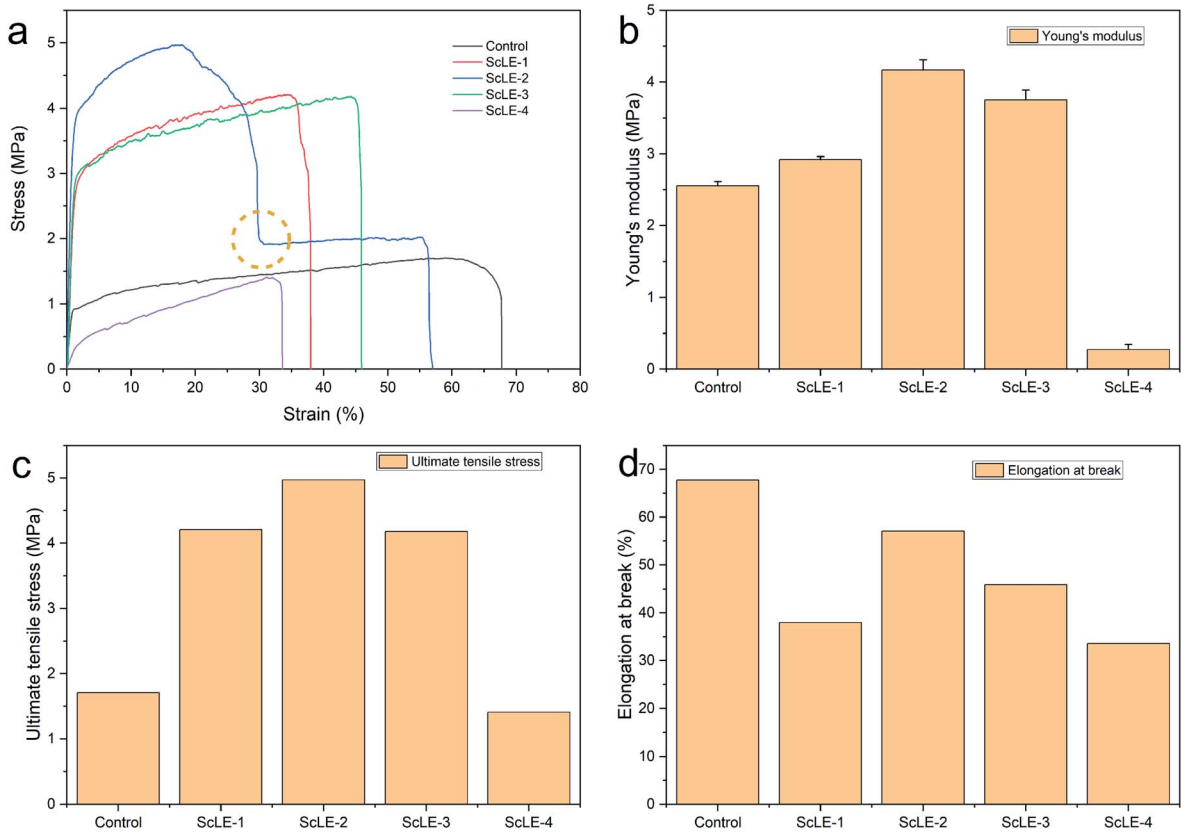

Fig. 5 (a) Stress–strain curves, (b) Young's moduli, (c) ultimate tensile stresses and (d) elongations at break for the neat PCL/PVP microfiber mesh and the PCL/PVP microfiber meshes containing ScLE.

The ultimate tensile strengths of ScLE-1 and ScLE-3 coincided with neat PCL/PVP microfiber mesh. Neat PCL/PVP microfibers had superior toughness and softness, and their failure stretch ratio reached 67.76%. The change trend in elongation at break of the prepared PCL/PVP microfiber mesh was consistent with the fiber diameter distribution in SEM, which indicated that the effect of ScLE on the elongation at break of the PCL/PVP microfibers was closely related to the fiber diameter. It is worth noting that although severe deformation or partial fracture in the ScLE-2 occurred in the tensile process, it could still adapt to the subsequent tensile process by reducing the tensile stress and avoid complete fracture to a certain extent, which represented outstanding tear resistance. This may contribute to the helical structure of most fibers in ScLE-2 and the "broken lotus root but joined fibers" effect obtained in the tensile process,[52] which further displayed the high strength and toughness of ScLE-2. In contrast, the poor mechanical properties of ScLE-4 were ascribed to the unstable fiber morphology caused by the poor interaction between excessive ScLE components and polymer molecules.

3.6. Hydrophobic–hydrophilic properties of the PCL/PVP microfibers

The water contact angle (WCA) can reflect the hydrophilic and hydrophobic properties of materials. Although PCL has good cell adhesion and proliferation effects, PCL is water-insoluble and a typical hydrophobic polymer, which limits the application of PCL in biomedicine. Typically, PVP is mixed with PCL to improve the hydrophilicity of the fibers.[28,32,38] Fig. 6a shows the WCA of the PCL/PVP microfibers prepared with different ScLE concentrations. The WCA of the microfiber membranes without ScLE was less than 10°, and their surfaces showed good hydrophilicity, which coincided with the high hydrophilicity of PCL fibers with added PVP in a previous report.[29] When ScLE was incorporated into the spinning solution, the WCA of the PCL/PVP microfibers sharply increased to about 90°. The WCA of the PCL/PVP microfibers slightly increased with the increase of the ScLE proportion. The water contact angle of 90° was the dividing line between hydrophilicity and hydrophobicity. The ScLE-1, ScLE-2 and ScLE-3 microfibers represented intermediate states between hydrophilicity and hydrophobicity, which would aid their application in biomedicine. Meanwhile, the hydrophobicity was also of benefit to the antibacterial activity and slow degradation of the microfibers.[53,54] Many hydrophobic components in ScLE improved the hydrophobicity of the microfiber membranes, and trace amounts of the hydrophilic components in ScLE were inserted between the PCL and PVP molecules to form hydrogen bonds with the carbonyl oxygen of PVP; this greatly reduced the effect of the hydrophilic groups, namely lactam bonds, in PVP. The methylene groups of the alkane chain and the pyrrolidone ring in PVP are hydrophobic groups, which twined around the hydrophilic zone composed of

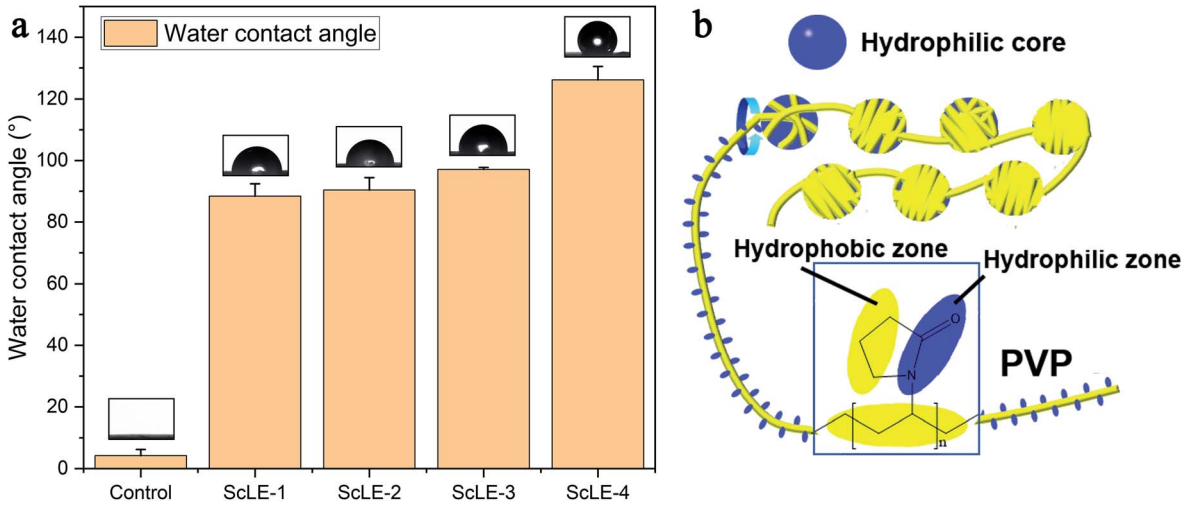

Fig. 6 (a) Static water contact angles of the neat PCL/PVP microfiber mesh and the PCL/PVP microfiber meshes containing ScLE and (b) schematic of the interaction between PVP and the hydrophilic components in ScLE.

hydrophilic components and lactams to form a linear structure, just as DNA tightly wraps around histones (Fig. 6b). Additionally, the winding structure had similar mechanical characteristics to a helix structure during the stretching process, which could store more stress as potential energy.[55,56] Therefore, the outstanding mechanical properties of ScLE-2 indirectly confirmed the existence of winding structure in the microfibers (Fig. 5).

3.7. *In vitro* degradation of the prepared microfibers

As tissue engineering materials, the degradation rate of fibers is an important design factor. The space supported by fibers can

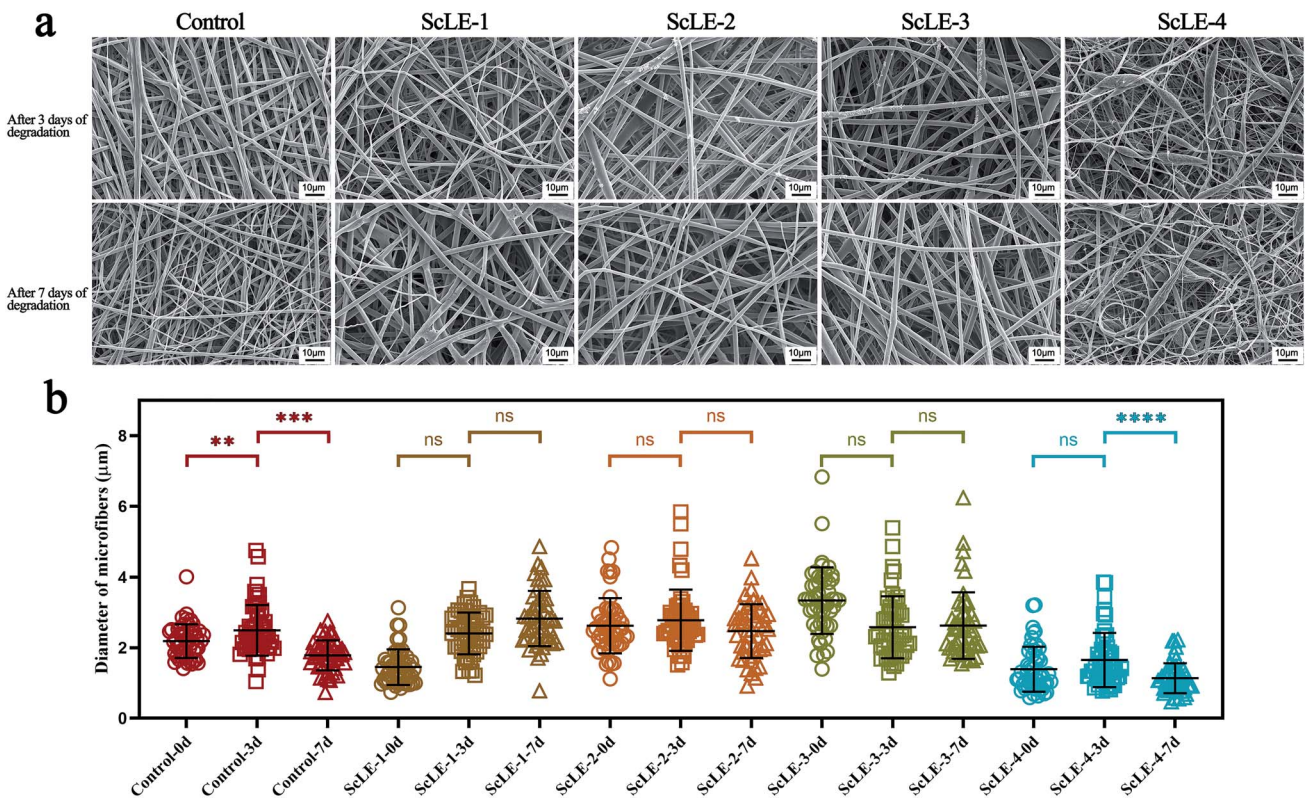

Fig. 7 (a) SEM images and (b) statistical results of electrospun fibers treated with PBS solution. p values of <0.05 were considered to be statistically significant: **, $p < 0.01$; ***, $p < 0.001$; ****, $p < 0.0001$. ns, $p > 0.05$, which indicates no significant difference among the two groups. The circles represent the microfibers in the initial state, and the squares and the triangles indicate that the microfibers are soaked in PBS solution for 3 days and 7 days, respectively.

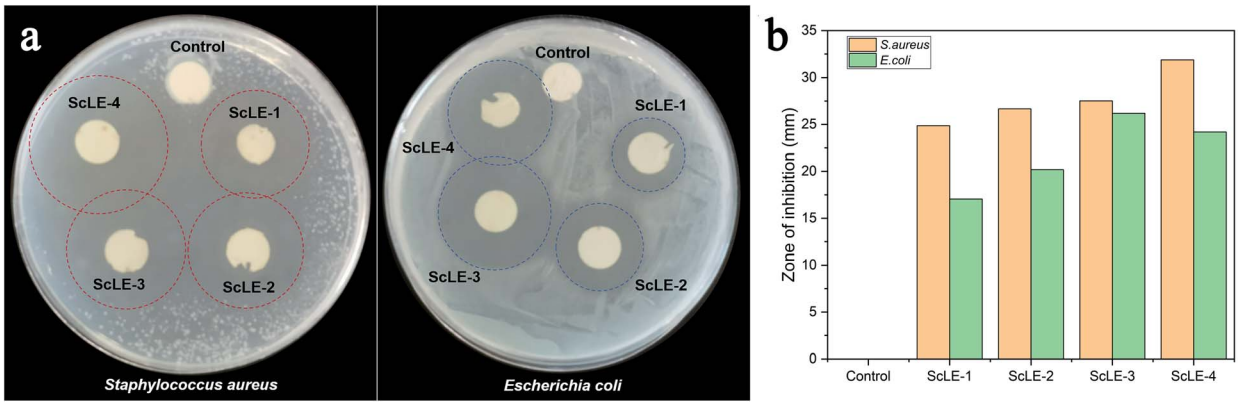

Fig. 8 (a) Antibacterial activity test and (b) results analysis of the neat PCL/PVP microfiber mesh and the PCL/PVP microfiber meshes containing ScLE.

maintain matrix deposition and tissue ingrowth in order to ameliorate the quality and quantity of regenerated tissue.[32] Meanwhile, the fibers also should have capability of retaining a stable structure and resisting the erosion of water vapor and salt for application in air purification. Fig. 7a shows the changes of the morphology of the fibers after treatment with PBS solution for 3 days and 7 days. After 3 days of treatment, the surface of the neat PCL/PVP microfibers was smooth, and there was no significant change compared with the surface before treatment. A few burrs appeared on the surface of ScLE-1. The burrs on ScLE-2 and ScLE-3 increased incrementally with the increase of the ScLE proportion, demonstrating that ScLE was being released at an accelerated rate. However, the fiber morphology of ScLE-4 did not seem to change; the reason for this may be that excessive ScLE significantly enhanced the hydrophobicity of the fibers to resist the erosion of PBS.[57,58] The morphology of the neat PCL/PVP microfibers remained unchanged after treatment for 7 days. There were some adherents on the surface of ScLE-1, which may be the result of partial swelling of the fibers. The burrs of ScLE-2 and ScLE-3 disappeared gradually, indicating that the fiber morphology recovered and the structure was stable after the release of ScLE. Similar to ScLE-1, ScLE-4 displayed a large number of adherents on the surface of the fibers and beads, which illustrated that the structure began to disintegrate. According to the statistical results of the fiber diameters in Fig. 7b, it could be confirmed that the neat PCL/PVP microfibers experienced the process of swelling and thickening first, followed by dissolving and thinning from outside to inside. There was no statistical difference in diameter after ScLE-1, ScLE-2 and ScLE-3 were treated with PBS for 3 days and 7 days, which showed that the ScLE addition improved the hydrophobicity of the fibers and effectively resisted the erosion and degradation of PBS solution to the fibers. It is noteworthy that the fiber diameter of ScLE-4 decreased significantly after 7 days of PBS treatment, manifesting the occurrence of degradation, which was consistent with the situation reflected in Fig. 7a. Although excessive ScLE increased the hydrophobicity of the fiber surface, it also led to an unstable structure (fibers-beads), which was more likely to cause the fibers to disintegrate in PBS solution.

3.8. Antibacterial activity test

The antibacterial activity of the neat PCL/PVP microfibers and PCL/PVP microfibers loaded with ScLE was assessed using the disc diffusion test against Gram-positive (*S. aureus*) and Gram-negative (*E. coli*) bacteria. The results of the antibacterial activity test are shown in Fig. 8. There was no transparent zone of inhibition around the pure PCL/PVP microfiber disc, demonstrating that it did not have any antibacterial activity against *S. aureus* or *E. coli*. Meanwhile, the PCL/PVP microfiber disc prepared with ScLE as the electrospinning solvent revealed excellent antibacterial properties. The antibacterial activity of ScLE-loaded PCL/PVP microfibers against *S. aureus* was enhanced with the increase of the ScLE proportion (Fig. 8b). Additionally, the active ingredients of ScLE diffusing from the PCL/PVP microfiber disc at the edge of the inhibition zone overlapped with each other, resulting in transparent areas outside the inhibition zone. This showed that ScLE exhibited good antibacterial effects on *S. aureus* and that ScLE had excellent migration and diffusivity. It was reported that *Cupressus* essential oil could kill microorganisms in the air, which could be applied in commercial air purification.[59] The inhibition effects of ScLE-loaded PCL/PVP microfibers against *E. coli* increased with increasing ScLE ratio up to ScLE-3 (Fig. 8b). The inhibition zone of ScLE-4 to *E. coli* was smaller than that of ScLE-3, which may be due to the instability of the bead structure in ScLE-4 and the excessive volatilization of active components in the sample in the process of sample preservation and the experiment. These results suggest that the morphology of the fibers is crucial to affect the performance of antibacterial agents with strong migration and diffusivity.

4. Conclusions

Electrospun ScLE-loaded PCL/PVP microfibers were successfully prepared by adding the extracts of *Sabina chinensis* leaves extracted with DCM and DMF at ambient temperature. The hydrophilic components in ScLE interacted with the PVP macromolecules to form a winding structure, which promoted the aggregation of microcrystals during electrospinning of the PCL/PVP solution and enhanced the surface hydrophilicity of

the microfibers. Simultaneously, this winding structure could store the stress as potential energy, displaying excellent mechanical properties. The hydrophilic and hydrophobic components in ScLE were effectively encapsulated by this winding structure to improve the thermal stability and degradation resistance of the fibers. ScLE-loaded PCL/PVP microfibers showed excellent antibacterial activity for both Gram-positive and Gram-negative bacteria, and the inhibition effect was stronger on Gram-positive bacteria. The ScLE-2 microfibers were considered better, as this sample presented better morphological, surface, thermal and tear resistance properties; hence, they are recommended for further production of microfibers. They can be applied in biomedical and air purification fields as antibacterial fiber materials.

Conflicts of interest

There are no conflicts to declare.

Acknowledgements

This work was supported by National Natural Science Foundation of China (grant number 51803095), Natural Science Foundation of Jiangsu Province in China (grant number BK20190927), Large Instruments Open Foundation of Nantong University (grant number KFJN2011).

References

1 X. G. Hu, H. Liu, J. Q. Zhang, Y. Q. Sun, Y. Q. Jin, W. Zhao, Y. A. El-Kassaby, X. R. Wang and J. F. Mao, *Mol. Breed.*, 2016, **36**, 99.
2 Y. Gao, Y. J. Jin, H. D. Li and H. J. Chen, *J. Integr. Plant Biol.*, 2005, **47**, 499–507.
3 H. C. Peng, *Guihaia*, 1992, **12**, 191–192.
4 D. Hao, Y. Zhang, H. Dai and Y. Wang, *Chromatography*, 2006, **24**, 185–187.
5 S. J. Kim, J. Y. Jung, H. W. Kim and T. Park, *Biol. Pharm. Bull.*, 2008, **31**, 1415–1421.
6 R. S. Darwish, H. M. Hammoda, D. A. Ghareeb, A. S. A. Abdelhamid, E. M. Bellah El Naggar, F. M. Harraz and E. Shawky, *J. Ethnopharmacol.*, 2020, **259**, 112971.
7 J. F. Carroll, N. Tabanca, M. Kramer, N. M. Elejalde, D. E. Wedge, U. R. Bernier, M. Coy, J. J. Becnel, B. Demirci, K. H. Baser, J. Zhang and S. Zhang, *J. Vector Ecol.*, 2011, **36**, 258–268.
8 A. M. Ali, M. M. Mackeen, I. Intan-Safinar, M. Hamid, N. H. Lajis, S. H. el-Sharkawy and M. Murakoshi, *J. Ethnopharmacol.*, 1996, **53**, 165–169.
9 Y. Q. Cui, P. Nan, M. H. Lin, J. Duan and X. H. Cui, *J. Environ. Health*, 2006, **23**, 63–65.
10 J. G. Wang, C. C. Xu, Y. K. Wong, Y. J. Li, F. L. Liao, T. L. Jiang and Y. Y. Tu, *Engineering*, 2019, **5**, 32–39.
11 M. Sherry, C. Charcosset, H. Fessi and H. Greige-Gerges, *J. Liposome Res.*, 2013, **23**, 268–275.
12 Y. Chen, M. Shafiq, M. Liu, Y. Morsi and X. Mo, *Bioact. Mater.*, 2020, **5**, 963–979.
13 S. Castro Coelho, B. Nogueiro Estevinho and F. Rocha, *Food Chem.*, 2021, **339**, 127850.
14 S. Fahimirad, Z. Fahimirad and M. Sillanpaa, *Sci. Total Environ.*, 2021, **751**, 141673.
15 W. B. Huang, Z. Y. Tong, R. Z. Wang, Z. J. Liao, Y. X. Bi, Y. Chen, M. L. Ma, P. Lyu and Y. Ma, *Ceram. Int.*, 2020, **46**, 26441–26453.
16 X. L. Lang, S. Gopalan, W. L. Fu and S. Ramakrishna, *Bull. Chem. Soc. Jpn.*, 2021, **94**, 8–20.
17 S. Mahalingam, R. Matharu, S. Homer-Vanniasinkam and M. Edirisinghe, *Appl. Phys. Rev.*, 2020, **7**, 041302.
18 X. X. Wang, G. F. Yu, J. Zhang, M. Yu, S. Ramakrishna and Y. Z. Long, *Prog. Mater. Sci.*, 2021, **115**, 100704.
19 X. R. Xie, Y. J. Chen, X. Y. Wang, X. Q. Xu, Y. H. Shen, A. U. R. Khan, A. Aldalbahi, A. E. Fetz, G. L. Bowlin, M. El-Newehy and X. M. Mo, *J. Mater. Sci. Technol.*, 2020, **59**, 243–261.
20 F. Notario-Perez, R. Cazorla-Luna, A. Martin-Illana, J. Galante, R. Ruiz-Caro, J. das Neves and M. D. Veiga, *J. Controlled Release*, 2020, **327**, 477–499.
21 T. S. Vo, M. M. Hossain, H. M. Jeong and K. Kim, *Nano Convergence*, 2020, **7**, 36.
22 M. Janmohammadi and M. S. Nourbakhsh, *Int. J. Polym. Mater. Polym. Biomater.*, 2019, **68**, 527–539.
23 S. Konchada, N. Killi, S. Sayyad, G. B. Gathalkar and R. V. N. Gundloori, *RSC Adv.*, 2020, **10**, 42827–42837.
24 S. J. Cho, S. M. Jung, M. Kang, H. S. Shin and J. H. Youk, *Polymer*, 2015, **69**, 95–102.
25 F. J. Camarena-Maese, F. Martinez-Hergueta, J. P. Fernandez-Blazquez, R. W. Kok, J. Reid and A. Callanan, *Polymer*, 2020, **203**, 122775.
26 M. O. Christen and F. Vercesi, *Clin., Cosmet. Invest. Dermatol.*, 2020, **13**, 31–48.
27 D. S. Chan, N. Fnais, I. Ibrahim, S. J. Daniel and J. Manoukian, *Int. J. Pediatr. Otorhinolaryngol.*, 2019, **123**, 38–42.
28 G. M. Kim, K. H. Le, S. M. Giannitelli, Y. J. Lee, A. Rainer and M. Trombetta, *J. Mater. Sci.: Mater. Med.*, 2013, **24**, 1425–1442.
29 Y. T. Jia, X. Y. Zhu and Q. Q. Liu, *Adv. Mater. Res.*, 2011, **332–334**, 1330–1334.
30 P. Franco and I. De Marco, *Polymers*, 2020, **12**, 12051114.
31 M. B. Gebeyehu, Y. H. Chang, A. K. Abay, S. Y. Chang, J. Y. Lee, C. M. Wu, T. C. Chiang and R. I. Murakami, *RSC Adv.*, 2016, **6**, 54162–54168.
32 R. PranavKumar Shadamarshan, H. Balaji, H. S. Rao, K. Balagangadharan, S. Viji Chandran and N. Selvamurugan, *Colloids Surf., B*, 2018, **171**, 698–706.
33 Y. T. Jia, C. Wu, F. C. Dong, G. Q. Huang and X. H. Zeng, *Appl. Mech. Mater.*, 2013, **268–270**, 580–583.
34 R. Li, Z. Q. Cheng, X. B. Yu, S. Wang, Z. L. Han and L. J. Kang, *Mater. Lett.*, 2019, **254**, 206–209.
35 N. Charernsriwilaiwat, T. Rojanarata, T. Ngawhirunpat and P. Opanasopit, *Int. J. Nanosci.*, 2016, **15**, 1650005.
36 S. Suganya, T. S. Ram, B. S. Lakshmi and V. R. Giridev, *J. Appl. Polym. Sci.*, 2011, **121**, 2893–2899.

37 Y. T. Jia, G. Huang, F. C. Dong, Q. Q. Liu and W. L. Nie, *Polym. Compos.*, 2016, **37**, 2847–2854.
38 X. H. Liu, S. D. Zheng, W. H. Dan and N. H. Dan, *Fibers Polym.*, 2016, **17**, 1186–1197.
39 M. Hashmi, S. Ullah and I. S. Kim, *Mater. Today Commun.*, 2020, **24**, 101161.
40 H. Y. Cui, M. Bai, C. Z. Li, R. K. Liu and L. Lin, *LWT–Food Sci. Technol.*, 2018, **96**, 671–678.
41 Y. Ge, J. Tang, H. Fu and Y. Fu, *J. Appl. Polym. Sci.*, 2020, **138**, e49670.
42 N. Joy, R. Anuraj, A. Viravalli, H. N. Dixit and S. Samavedi, *Chem. Eng. Sci.*, 2021, **230**, 116200.
43 S. S. S. Bakar, K. M. Foong, N. A. Halif and S. Yahud, *IOP Conf. Ser.: Mater. Sci. Eng.*, 2019, **701**, 012018.
44 D. Deshawar, K. Gupta and P. Chokshi, *Polymer*, 2020, **202**, 122656.
45 S. Maghsoodlou, B. Noroozi and A. K. Haghi, *Nano*, 2017, **12**, 1750028.
46 J. H. Kim, H. Lee, A. W. Jatoi, S. S. Im, J. S. Lee and I. S. Kim, *Mater. Lett.*, 2016, **181**, 367–370.
47 S. Ullah, M. Hashmi, N. Hussain, A. Ullah, M. N. Sarwar, Y. Saito, S. H. Kim and I. S. Kim, *J. Water Process. Eng.*, 2020, **33**, 101111.
48 Q. B. Yang, Z. Y. Li, Y. L. Hong, Y. Y. Zhao, S. L. Qiu, C. Wang and Y. Wei, *J. Polym. Sci., Part B: Polym. Phys.*, 2004, **42**, 3721–3726.
49 H. Y. Cui, C. H. Zhang, C. Z. Li and L. Lin, *Ind. Crops Prod.*, 2019, **140**, 111739.
50 X. D. Chen, *Small Methods*, 2017, **1**, 1600029.
51 G. Nallathambi, B. Robert, S. P. Esmeralda, J. Kumaravel and V. Parthiban, *Res. J. Text. Apparel*, 2020, **24**, 72–83.
52 Q. F. Guan, Z. M. Han, Y. Zhu, W. L. Xu, H. B. Yang, Z. C. Ling, B. B. Yan, K. P. Yang, C. H. Yin, H. Wu and S. H. Yu, *Nano Lett.*, 2021, **21**, 952–958.
53 Y. F. Yang, S. L. Zheng, Q. Liu, B. H. Kong and H. Wang, *Food Packaging and Shelf Life*, 2020, **26**, 100600.
54 H. L. Tan, D. Kai, P. Pasbakhsh, S. Y. Teow, Y. Y. Lim and J. Pushpamalar, *Colloids Surf., B*, 2020, **188**, 110713.
55 L. Wang, K. Cai, J. Shi and Q. H. Qin, *Appl. Surf. Sci.*, 2020, **527**, 146848.
56 S. Choudhary and A. J. Crosby, *J. Polym. Sci., Part B: Polym. Phys.*, 2019, **57**, 1270–1278.
57 H. L. Yu, W. H. Liu, D. M. Li, C. H. Liu, Z. B. Feng and B. Jiang, *Polymers*, 2020, **12**, 12071565.
58 L. Y. Huo, J. C. Luo, X. W. Huang, S. Zhang, S. J. Gao, B. Long and J. F. Gao, *Colloids Surf., A*, 2020, **603**, 125224.
59 S. H. Lee, H. S. Do and K. J. Min, *PLoS One*, 2015, **10**, e0143450.